Multistable and dynamic CRISPRi-based synthetic circuits

Javier Santos-Moreno and Yolanda Schaerli

Department of Fundamental Microbiology, University of Lausanne, Biophore Building, 1015 Lausanne, Switzerland

yolanda.schaerli@unil.ch

Abstract

Gene expression control based on CRISPRi (clustered regularly interspaced short palindromic repeats interference) has emerged as a powerful tool for creating synthetic gene circuits, both in prokaryotes and in eukaryotes; yet, its lack of cooperativity has been pointed out as a potential obstacle for dynamic or multistable circuit construction, raising the question of whether CRISPRi is widely applicable for synthetic circuit design. Here we use CRISPRi to build prominent synthetic gene circuits that accurately govern temporal and spatial gene expression in *Escherichia coli*. We report the first-ever CRSPRi oscillator ("CRISPRlator"), bistable network and stripe pattern-forming incoherent feed-forward loop (IFFL). Our circuit designs, conceived to feature high predictability and orthogonality and low metabolic burden and context-dependency, allowed us to achieve robust circuit behaviors (e.g. synchronous oscillations) and to expand the IFFL into a twice as complex, two-stripe patterning system. Our work demonstrates the wide applicability of CRISPRi in synthetic circuits and paves the way for future efforts towards engineering more complex synthetic networks, boosted by the advantages of CRISPR technology.

Introduction

Synthetic biology aims to build artificial decision-making circuits that are programmable, predictable and perform a specific function[1]. Since the rise of synthetic biology in the 2000s, most synthetic circuits have been governed by protein-based regulators. Recently, however, there has been growing interest in circuits based on RNA regulators as a means to overcome some of the intrinsic limitations of protein regulators[2].

The prokaryotic adaptive immunity system CRISPR constitutes a powerful platform for the construction of RNA-driven synthetic circuits[3]. The catalytically-dead mutant dCas9 can be easily

directed to virtually any sequence by a single-guide RNA molecule (sgRNA). When a prokaryotic promoter (or downstream) region is targeted, steric hindrance by the dCas9-sgRNA complex results in transcriptional repression – an approach known as CRISPR interference (CRISPRi). CRISPRi offers several advantages over protein regulators for synthetic circuit design. Due to its RNA-guided nature, CRISPRi is highly programmable[4,5], allows for easy design of sgRNAs that can be highly orthogonal[6] and whose behavior in different environments can be easily predicted *in silico*[7,8]. It also imposes low burden on host cells[2] and is encoded in shorter sequences than protein-based repressors, thereby facilitating circuit handling and delivery and reducing cost. A potential drawback of CRISPRi is the lack of non-linearity[9] of its dose-response functions. Cooperative protein transcription factors typically function non-linearly, a difference that might prevent the successful implementation of CRISPRi-based dynamic and multistable circuits[9-11]. Besides, unlike other RNA circuits that exhibit fast dynamics, low rates of dCas9:DNA dissociation in the absence of DNA replication[12,13] effectively slow down CRISPRi dynamics. Potential strategies to overcame such limitations and yield multistable and dynamic circuits have been proposed, and include the precise tuning of active dCas9 degradation, an increased CRISPRi fold-repression, faster dCas9:DNA binding[10], fusing dCas9 to additional repressor domains[14] or incorporating activators in the circuit design[11,15]. Alternatively, competition for dCas9[16] and cellular resources may render non-cooperative systems non-linear, as demonstrated for a T7 RNA polymerase-controlled positive feedback circuit[17].

The last few years have seen a growing interest in developing CRISPRi-based synthetic circuits[6,9,14,18-25]. However, despite the enormous potential of CRISPRi for synthetic circuit design, the use of CRISPRi circuits in prokaryotes has been largely focused on logic gates and to the best of our knowledge none of the flagship circuits in synthetic biology (namely, the bistable toggle-switch[26] and the repressilator[27]) have been re-constructed using CRISPRi. Here, we fill this unaddressed gap by demonstrating that CRISPRi can be used for building some of the most notorious (synthetic) circuit topologies: the repressilator, a bistable circuit, and an incoherent feed-forward loop (IFFL, a.k.a. band-pass filter) that drives stripe pattern formation.

Results and Discussion

Design features and CRISPRi testing.

To maximize circuit predictability and orthogonality and minimize metabolic burden on the host, we employed a series of design features in all our synthetic networks. Circuit components were all expressed from a single vector (so-called “variable” vector) to avoid fluctuations in their stoichiometry. Circuit transcriptional units (TUs) were isolated from each other by strong transcriptional terminators and 200 bp spacer sequences, to avoid transcriptional readthrough and minimize compositional context[28]. To prevent mRNA context-dependency and provide

transcriptional insulation within TUs, a 20 bp csy4 cleavage sequence[29] was used flanking sgRNAs and upstream of the ribosome binding sites (RBS) of the reporter genes. Orthogonal degradation tags[30] were used to avoid cross-talk between fluorescent reporters. Sequence repetition at the DNA level were minimized to prevent unwanted recombination events. The levels of dCas9 and Csy4 were kept constant by expressing them from constitutive promoters in a separate "constant" vector. All gene circuits were tested in *E. coli* (MK01[31]) incubated in a rich defined media (EZ, Teknova) for maximizing cell fitness while reducing variability. In order to speed up the design-build-test cycle, we adopted a previously-described cloning strategy that allows for fast and modular assembly of synthetic networks[32].

We first devised a simple circuit to assess the dose-response of CRISPRi repression. This 2-node network design displays Boolean NOT logic, in which node 1 (N1) is induced by L-arabinose (Ara) and represses expression of node 2 (N2) (Fig. 1). Levels of N1 and N2 in the NOT circuit were monitored *via* the fluorescent reporters mKO2 and sfGFP (Fig. 1b) carrying degradation tags (MarA and MarAn20) to accelerate reporter turnover[30]. We chose four single-guide RNAs (sgRNA-1 to -4) and their corresponding binding sites (bs-1 to -4), previously shown to be orthogonal to each other[6]. Maximal induction (0.2% Ara) of N1 produced sgRNA levels that repressed the expression of N2 in the range of 10 to 30-fold (Fig. 1c), with sgRNA-2 being the strongest repressor. Truncation of the four 5' nucleotides ("t4") of sgRNA-1 and -4 reduced maximal repression by 20% and 45%, respectively, providing a means to tune-down repression (Fig. 1c). We also measured N2 fluorescence in the presence of different Ara concentrations (Fig. 1d), which showed a modulable, dose-dependent CRISPRi repression, a prerequisite for building dose-dependent circuits.

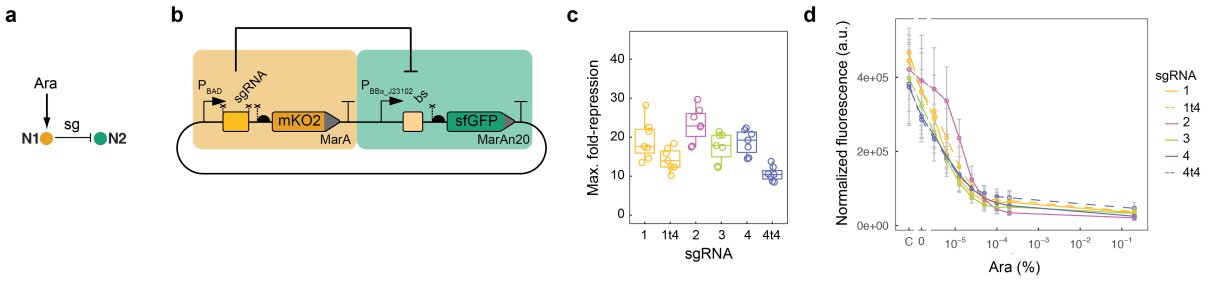

Fig. 1. Assessment of CRISPRi repression through a 2-node NOT logic circuit. (**a**) Schematic representation of the circuit architecture, where the first node (N1) is induced by Ara and in turn produces a sgRNA ("sg") that represses the second node (N2). (**b**) Details of the circuit design. In addition, AraC, dCas9 and Csy4 are constitutively expressed. Bent arrows: promoters; squares: sgRNA binding sites; rectangles: sgRNAs; crosses: csy4 recognition sites; semicircles: RBSs; pointed rectangles: reporter genes with degradation tags; and "T"-s: transcriptional terminators. (**c**) Maximum fold-repression of N2 achieved by four different sgRNAs, calculated as the GFP fluorescence of a fully-induced (0.2% Ara) circuit relative to a control lacking the sgRNA. Truncated

variants of sgRNA-1 and -4 lacking the four 5' nucleotides ("t4") were also assessed. Data corresponds to seven biological replicates. Boxes represent quartiles Q1 (box lower limit), Q2 (i.e. median, internal line) and Q3 (box upper limit); whiskers comprise data points that are no more than 1.5 x IQR (inter-quartile region, i.e. the length of the box) away from the box. (**d**) Dose-response curves for the NOT circuits operating through sgRNA-1 to -4 (including t4 variants of sgRNA-1 and -4). The response (GFP fluorescence) of all four circuits can be modulated by adjusting the input dose (Ara). The controls lacking the sgRNAs ("C") showcase some level of P_{BAD} leakiness in the NOT circuits that results in weak repression even in the absence of Ara ("0"). Mean and s.d. of three biological replicates.

A CRISPRi bistable circuit.

We next sought to build a classical genetic circuit that has never been constructed before using CRISPRi: a bistable circuit (BC)[26], where two nodes mutually repress each other resulting in two mutually-exclusive states. We designed a double-inducible BC in which each of the two nodes responds to a small molecule (Ara or N-(β-Ketocaproyl)-L-homoserine lactone, AHL) by producing a fluorescent reporter (mKO2-MarA or sfGFP-MarAn20) and a sgRNA (-1 or -4) that represses the other node (Fig. 2a and b). When BC bacteria were subjected to perpendicular gradients of Ara and AHL following pre-incubation in either one or the other inducer, they displayed different reporter expression profiles depending on the previous state (Fig. 2c), a phenomenon known as hysteresis that characterizes bistable systems like the toggle switch[26]. As expected, we identified three defined populations of BC cells according to the levels of orange (O) and green (G) reporters (Fig. 2c and Supplementary Fig. 1): lowO-lowG (at low Ara & low AHL), highO-lowG (at high Ara & low AHL), and lowO-highG (at low Ara & high AHL). Double induction (high Ara & high AHL) resulted in high levels of hysteresis: AHL pre-culture locked cells in the green state (Fig. 2c, middle), while Ara pre-culture yielded a mixed population of orange-only and green-only cells (Fig. 2c, left, and Supplementary Fig. 1). Indeed, flow cytometry analysis discarded the presence of orange-and-green cells under any condition and confirmed that the CRISPRi BC network is bistable (Supplementary Fig. 1). Control circuits with no repression (control C1) or a single repression (controls C2 and C3) showed no hysteresis (Supplementary Fig. 2). Together, these results show that CRISPRi can be applied to build multistable gene circuits.

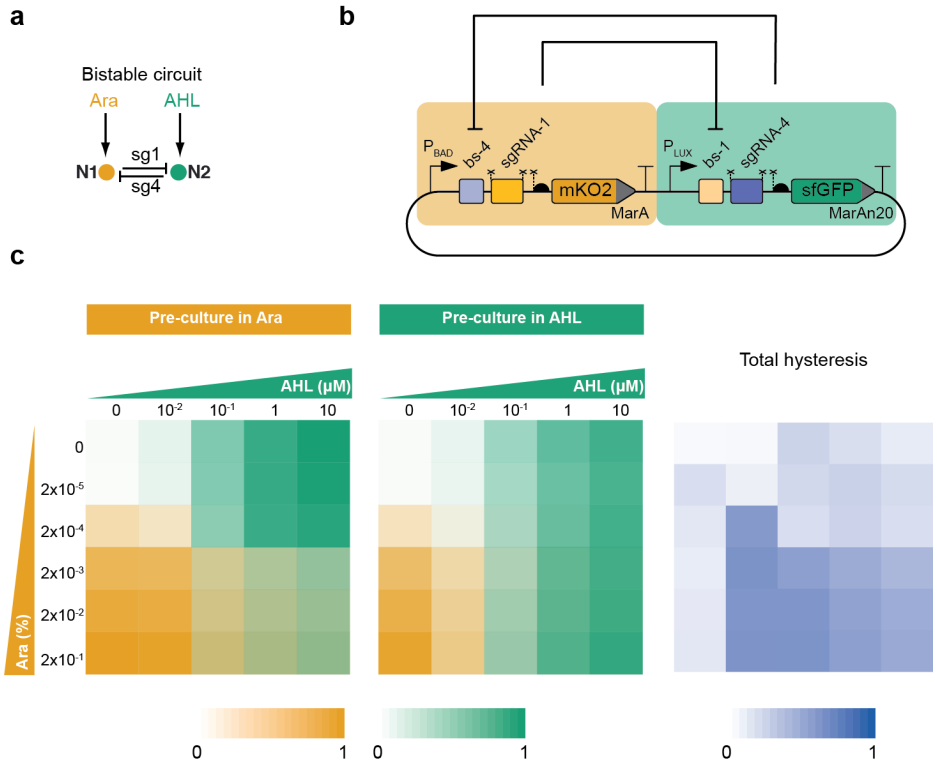

Fig. 2. The CRISPRi-based bistable circuit (BC). (**a**) Topology of the BC. (**b**) Molecular implementation. Symbols as described in Fig. 1. (**c**) Left and middle: Expression of the two fluorescent reporters, mKO2 (orange) and sfGFP (green), when subjected to the indicated amounts of the inducers (Ara and AHL). Right: total hysteresis calculated as the difference in reporter expression between the two pre-incubation conditions (see Methods).

CRISPRi incoherent feed-forward loops.

We next decided to build another flagship synthetic circuit, a stripe-forming IFFL (Fig. 3)[33-35]. We designed a CRISPRi-based 3-node IFFL type 2 (I2), which relies exclusively on repression interactions[36]. To monitor the behavior of all three nodes of the circuit, we employed compatible fluorescent reporters fused to orthogonal degradation tags[30]: mKO2-MarA, sfGFP-MarAn20 and RepA70-mKate2 (Fig. 3b). The rationally designed circuit performed as expected: with increasing Ara levels N1 levels raised, resulting in a concomitant decrease of N2; a peak (stripe) of N3 was observed in the *open window* between N1 and N2 (Fig. 3c). To our knowledge, this is the first example of an IFFL endowed with three reporters, which allowed us to readily monitor network behavior and to optimize it – and to use the circuit as a concentration-detector (Supplementary Fig. 3). The inclusion of three reporter protein-coding genes was enabled by the small size and transcriptional nature of the circuit, causing low burden on host cells. Even more, due to the relatively small size of the circuit in terms of DNA sequence, all 3 nodes of the network could be carried within a single plasmid, thus keeping their relative abundance constant and avoiding

fluctuations in their stoichiometry due to plasmid copy number variations. To corroborate that the CRISPRi IFFL was capable of true spatial patterning, we homogeneously spread bacteria on an agar plate and applied a central source of arabinose, which diffused forming a radial gradient. Consistent with the French flag model[37], the initially identical, isogenic bacterial population carrying the synthetic network interpreted the Ara gradient into three discrete gene expression programs: “orange”, “green” and “blue” (Fig. 3d).

We next wanted to explore the robustness of the CRISPRi stripe circuit with respect to variations in its molecular components. We assessed the performance of i) a circuit carrying a single reporter (sfGFP-MarAn20 in N3), ii) a circuit with a different set of sgRNA regulators (sgRNA-4, sgRNA-4t4 and sgRNA-3 instead of sgRNA-1, sgRNA-1t4 and sgRNA-2), and iii) a network with swapped N2 and N3 reporters (Supplementary Fig. 4). All these circuits showed a stripe behavior (Supplementary Fig. 4), demonstrating the robustness of our CRISPRi-based IFFL, which is enabled by our design aiming at high orthogonality and low context-dependency.

An important limitation that commonly affects synthetic gene circuits is the difficulty to expand their functionality by including existing circuits into more complex networks or by making them operate in a different environment, such as in co-existence with another circuit. To test whether a CRISPRi-based IFFL could operate in a similar manner in a different context, we decided to build two orthogonal CRISPRi IFFLs that would operate in parallel within the same bacterial cell, each producing a single (and independent) stripe in response to a common arabinose gradient (Fig. 3e). When bacteria containing both parallel circuits were submitted to different Ara concentrations, a double peak of gene expression could be observed at intermediate inducer levels corresponding to two overlapping peaks, each generated by one of the circuits, as designed (Fig. 3f). To our knowledge, this is the first study reporting a double synthetic stripe driven by a single (isogenic) cell population. The simultaneous yet independent operation of the double-stripe system was enabled by the intrinsic properties of CRISPRi (orthogonality, low burden, short encoding sequences) and the low context-dependency of the design.

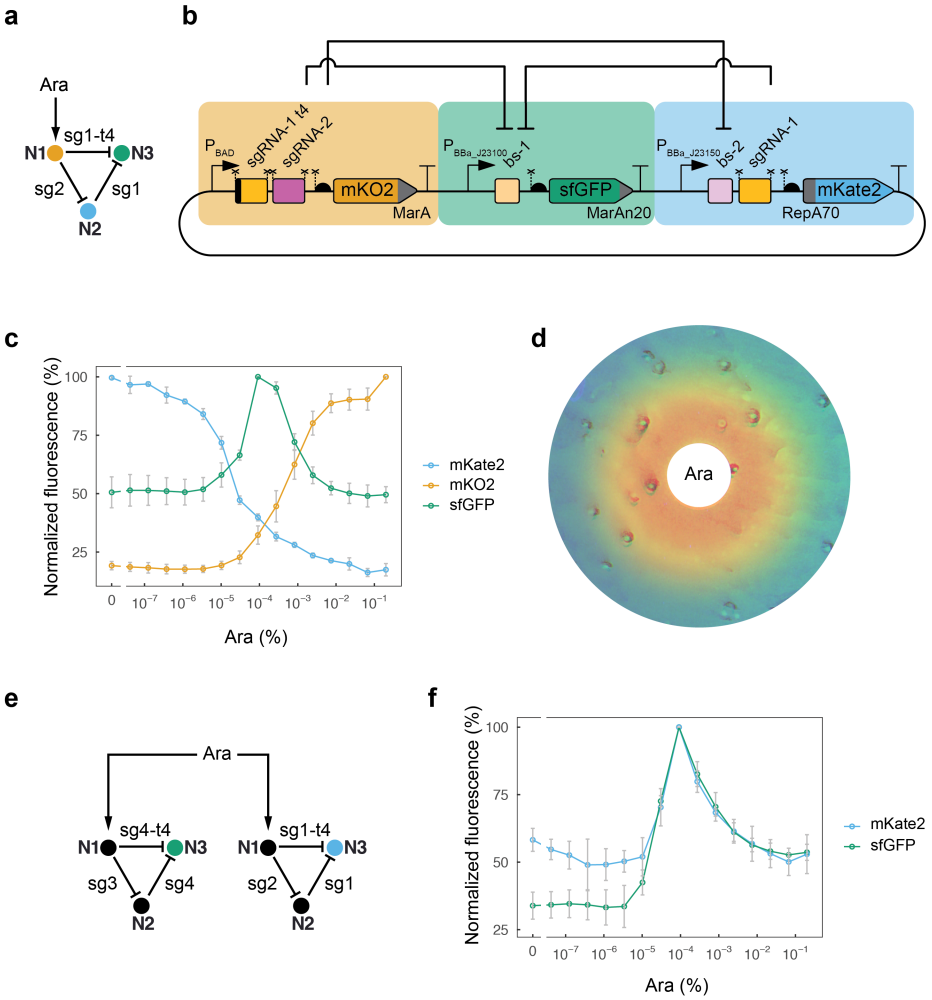

Fig. 3. Stripe-forming synthetic IFFL based on CRISPRi. (**a**) I2 topology of the circuit design. (**b**) Molecular implementation of the synthetic CRISPRi IFFL. Symbols as described in Fig. 1. (**c**) Behavior of the network (output) as a function of inducer concentration (input). Fluorescence of the three nodes was recorded and plotted together. Mean and s.d. of three biological replicates. (**d**) Spatial pattern formation by the artificial CRISPRi circuit. Bacteria carrying the synthetic network were plated homogeneously on agar and a paper disk soaked with Ara was placed in the center of the plate (white), creating a radial Ara gradient by diffusion. The initially identical isogenic population developed a 3-domain pattern in which each domain is characterized by differentially expressed genes. Orange, mKO2; green, sfGFP; blue, mKate2. Note that false colors were chosen for mKO2 (emission λ 565 nm) and mKate2 (emission λ 633 nm) to highlight differences between the two. (**e**) Topology of the two-IFFL system. (**f**) Double-stripe phenotype displayed by bacteria carrying the two parallel but independent CRISPRi stripe networks (two-IFFL system). Mean and s.d. of three biological replicates.

Next, we designed an IFFL in which both the control and the reporting are RNA-based. To this aim, we modified our CRISPRi IFFL (in which the control is sgRNA-based) to remove the

"orange" and "blue" reporters and substituted the original "green" reporter (sfGFP) with 8 copies of the dBroccoli (dimeric Broccoli) RNA aptamer[38] (Supplementary Fig. 5). When we incubated the engineered bacteria with the DFHBI-1T fluorophore we observed a low-background Broccoli stripe (Supplementary Fig. 5b), showing that the band-pass behavior of an RNA-controlled IFFL can indeed be reported by an RNA molecule.

The CRISPRlator: a CRISPRi oscillator.

Finally, we wanted to explore whether CRISPRi-based circuits could be employed not only for spatial patterning, as demonstrated above, but also to create temporal patterns. Oscillations are temporal patterns with key roles in many different biological phenomena. We sought to engineer an oscillatory pattern controlled by a dynamic CRISPRi circuit. To this aim, we designed a 3-node ring oscillator: the "CRISPRlator" (Fig. 4), in honor of the first synthetic oscillator (the repressilator)[27]. Bacteria carrying the CRISPRlator were grown in a continuous culture within a microfluidic device (Supplementary Fig. 6) for 3 days (over 100 generations) and imaged every 10 min. The CRISPRlator generated robust oscillations between three states ("red", "green" and "blue") with a period of 10-12 h (14-17 generations, Fig. 4c and d). Oscillations were synchronized at the population level (~110 cells per chamber) for hundreds of generations even in the absence of any engineered synchronization mechanism (Supplementary Movie 1) and can thus rival the optimized versions of the protein-based repressilator[39,40].

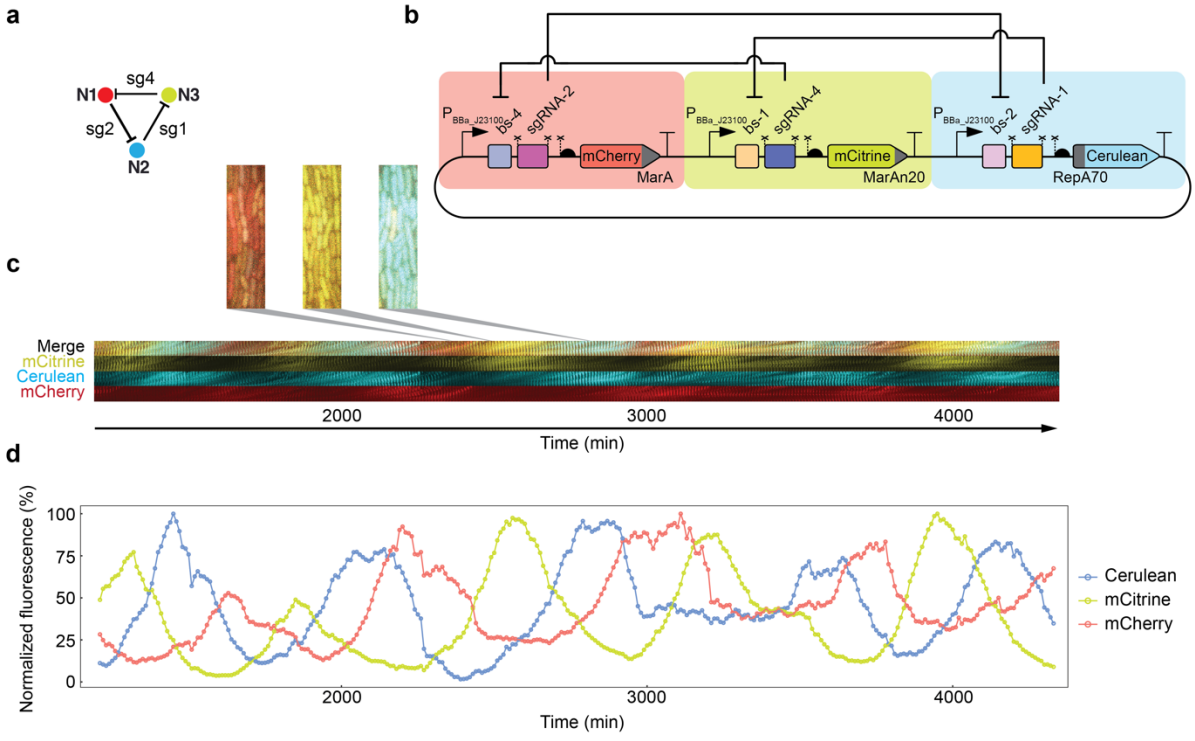

Fig. 4. The CRISPRlator, a CRISPRi-based oscillator. (**a**) Topology of the ring oscillator. (**b**) Molecular implementation of the CRISPRlator. Symbols as described in Fig. 1. (**c**) Montage showing the oscillations of the three fluorescent reporters over time. Bacteria were grown in continuous exponential phase in a microfluidic device for 3 days and imaged every 10 min. Microscopy images (as those enlarged in the zoom-ins) are displayed together in a "timeline" montage (kymograph). (**d**) Quantification of the population-level fluorescence of ~110 cells over time. Oscillations display a period of 10-12 h.

Together, our results demonstrate that the lack of cooperativity of CRISPRi is not an insurmountable obstacle for (complex) synthetic circuit construction and CRISPRi can effectively be used for generating dynamic and multistable behaviors. Future work will reveal the source of non-linearity in these circuits. The benefits inherent to CRISPRi circuits will likely prompt the construction of new/extended versions of the BC and the CRISPRlator, including designs hard to achieve with protein repressors, e.g. two independent clocks operating within the same cell. The universality of CRISPR should facilitate the transfer of our circuits into other species. We anticipate that our results will encourage the synthetic biology community to employ CRISPRi for gene circuit design and inspire future construction of more complex synthetic networks.

Methods

Circuit construction.

Genes encoding sfGFP, mKO2, mKate2, Csy4 and dCas9 were obtained as previously described[32]. mCherry and mCitrine were amplified from plasmids (pLacI(r)-mCherry(ASV) and pCI-Citrine-(ASV)) kindly provided by Sebastian Maerkl[39]. dBroccoli was amplified from plasmid pET28c-F30-2xdBroccoli, which was a gift from Samie Jaffrey (Addgene plasmid #66843). Cerulean[41] was purchased as an *E. coli* codon-optimized gBlock from IDT, and LuxR (BBa_C0062) was also codon-optimized and synthesized by GenScript. Primers were purchased desalted from Microsynth or Sigma-Aldrich. The circuits were constructed employing a previously described Gibson-based cloning framework that allows for the fast and modular cloning of synthetic gene networks[32]. Plasmids used in this study (Supplementary Table 1) are available through Addgene.

Microplate reader experiments.

Gene expression of fluorescent reporters was used to assess synthetic circuit performance; fluorescence was measured in microplate readers (except for the agar plate experiment in Fig. 3d and the microfluidic experiment in Fig. 4). MK01[31] electrocompetent cells were transformed with a

"constant" plasmid encoding proteins required for circuit function (namely dCas9 and Csy4, plus LuxR when applicable) as well as with a "variable" vector bearing AraC (when needed) and the CRISPRi circuit (see Supplementary Table 1 for a detailed plasmid description). 2 ml of selective LB (plus 0.2% Ara or 10 µM AHL in the case of the CRISPRi BC) were inoculated with single colonies and incubated at 37° C for ~6 h; cells were pelleted at 4000 rcf and resuspended in selective EZ medium (Teknova) with 0.4% glycerol. 120 µl of 0.05 OD_{600} bacterial suspensions (or 0.001 OD_{600} for the bistable circuit) were added per well on a 96-well CytoOne plate (Starlab), and 2.4 µl of the corresponding inducer (L-arabinose or N-(β-Ketocaproyl)-L-homoserine lactone (AHL), Sigma) were added to yield the indicated concentrations. Plates were incubated at 37° C with double-orbital shaking in a Synergy H1 microplate reader (Biotek). Fluorescence was determined after 16 h (for protein reporters) or 6 h (for Broccoli RNA reporter) with the following settings: mKO2: Ex. 542 nm, Em. 571 nm; sfGPF: Ex. 479 nm, Em. 520 nm; mKate2: Ex. 588 nm, Em. 633 nm. For the Broccoli RNA aptamer, 40 µM DFHB1-1T (Tocris Bioscience) were added to the medium. Fluorescence levels were treated as follows: i) the fluorescence signal in a blank sample was subtracted, ii) the resulting value was divided by the absorbance at 600 nm to correct for differences in bacterial concentration, and finally iii) the bacterial auto-fluorescence of a strain with no reporter genes was subtracted. Subsequently, corrected fluorescence was normalized to a percentage scale by dividing all values of a given color by the highest value of that color. For hysteresis calculation, the difference between the normalized fluorescence of the two pre-incubation conditions (pre-culture in Ara and pre-culture in AHL) was computed for each condition (i.e. unique combination of Ara and AHL), and divided by the maximum normalized fluorescence of the corresponding condition. This was done for mKO2 and sfGFP separately, after which values for both reporters were added and divided by two to yield the total hysteresis in a scale from 0 to 1.

Flow cytometry.

Bacteria carrying the BC network were pre-cultured (~6 h) and cultured (16 h) as stated above, diluted 1:200 in phosphate-buffered saline (PBS) and analyzed with a BD LSRFortessa flow cytometer using a 488 nm laser in combination with FITC filter for sfGFP and a 561 nm laser with a PE-Texas Red filter for mKO2. 10'000 events were acquired with BD FACSDiva 6.2 software. Bacterial cells were gated in the FSC-H vs SSC-H plot using FlowJo (FlowJo, LLC) and plotted using R[42].

Agar plate assay.

MK01[31] electrocompetent cells were transformed with the "constant" plasmid pJ1996_v2[32], which carries dCas9 and Csy4, and a "variable" plasmid encoding the three-color IFFL (pJ2042.2). 2 ml

of selective LB were inoculated with single cells and grown at 37° C for ~6 h; cells were pelleted at 4000 rcf and resuspended in selective EZ medium (Teknova) with 0.4% glycerol. 300 µl of 0.15 OD_{600} bacterial suspensions were added to pre-warmed (1 h 37° C) Petri dishes containing selective EZ medium (Teknova) with 0.4% glycerol and 0.9% agar, and suspensions were spread with sterile glass beads. After incubating 1 h at 37° C, a filter paper disk was placed in the center of the agar, and 15 µl of 5% Ara were delivered onto the disk. Plates were incubated at 37° C and imaged after 20 h with an Amersham Typhoon 5 Biomolecular Imager (GE Healthcare) using the following settings: mKO2: Ex. 532 nm, Em. 560-580 nm; sfGPF: Ex. 488 nm, Em. 515-535 nm; mKate2: Ex. 635 nm, Em. 655-685 nm. Grayscale images were converted to color images using Fiji[43] and overlaid.

Microfluidic experiments.

MK01[31] electrocompetent cells were transformed with the "constant" plasmid pJ1996_v2[32] and a "variable" plasmid encoding the CRISPRlator. Single colonies were used to inoculate 5 ml of selective LB, which were grown overnight at 37° C. Next morning, 3 ml of selective EZ containing 0.85 g/l Pluronic F-127 (Sigma) were inoculated with the overnight preculture in a 1:100 ratio and grown for 3-4 h at 37° C. Cells were centrifuged for 10 min at 4000 rcf and resuspended in ~10 µl of the supernatant to obtain a dense suspension, which was loaded into the PDMS microfluidics device. Cells were grown in a continuous culture inside microfluidic chambers (dimensions: 1.2 µm x 12 µm x 60 µm, h x w x l, purchased from Wunderlichips, see design in Supplementary Fig. 6) for 3 days with a constant 0.5 ml/h supply of fresh medium (selective EZ plus 0.85 g/l Pluronic F-127) and removal of waste and excess of bacteria, powered by an AL-300 pump (World Precision Instruments). Imaging was performed using a Leica DMi8 microscope and a Leica DFC9000 GT camera, with the following settings: Cerulean: Ex. 440 nm 10% 50 ms, Em. 457-483 nm; mCitrine: Ex. 510 nm 10% 50 ms, Em. 520-550 nm; mCherry: Ex. 550 nm 20% 200 ms, Em. 600-670 nm. Imaging started after 20 h to allow cells to fill the chamber and oscillations to stabilize, and images were collected every 10 min with LAS X software, and analyzed using Fiji[43] for both quantification and montage.

Author Contributions

JSM and YS designed research. JSM performed experiments, analyzed data, and prepared the figures. JSM and YS wrote the manuscript. All authors have given approval to the final version of the manuscript.

Conflict of Interest

The authors declare no conflict of interest.

Acknowledgments

We thank Imre Banlaki for cloning *luxR* gene into pJ1996_v2 to yield pJ2018.2, Içvara Barbier for help with microfluidics and feedback about bistable circuits, and Marc García-Garcerà for help with R language. We also thank Mariapia Chindamo, Florence Gauye, Virginie Kahabdian, Borany Kim and Léo Moser for excellent technical assistance; Marc Güell, Mark Isalan, and Jan-Willem Veening for critical reading of the manuscript, and all Schaerli lab members for useful discussions. This work was funded by Swiss National Science Foundation Grant 31003A_175608.

References

1 Xie, M. Q. & Fussenegger, M. Designing cell function: assembly of synthetic gene circuits for cell biology applications. *Nat. Rev. Mol. Cell. Bio.* **19**, 507-525, (2018).

2 Chappell, J., Watters, K. E., Takahashi, M. K. & Lucks, J. B. A renaissance in RNA synthetic biology: new mechanisms, applications and tools for the future. *Curr. Opin. Chem. Biol.* **28**, 47-56, (2015).

3 Jusiak, B., Cleto, S., Perez-Pinera, P. & Lu, T. K. Engineering Synthetic Gene Circuits in Living Cells with CRISPR Technology. *Trends Biotechnol.* **34**, 535-547, (2016).

4 Qi, L. S. *et al.* Repurposing CRISPR as an RNA-guided platform for sequence-specific control of gene expression. *Cell* **152**, 1173-1183, (2013).

5 Bikard, D. *et al.* Programmable repression and activation of bacterial gene expression using an engineered CRISPR-Cas system. *Nucleic Acids Res.* **41**, 7429-7437, (2013).

6 Didovyk, A., Borek, B., Hasty, J. & Tsimring, L. Orthogonal Modular Gene Repression in Escherichia coli Using Engineered CRISPR/Cas9. *ACS Synth Biol* **5**, 81-88, (2016).

7 Zuker, M. Mfold web server for nucleic acid folding and hybridization prediction. *Nucleic Acids Res.* **31**, 3406-3415, (2003).

8 Zadeh, J. N. *et al.* NUPACK: Analysis and design of nucleic acid systems. *J. Comput. Chem.* **32**, 170-173, (2011).

9 Nielsen, A. A. & Voigt, C. A. Multi-input CRISPR/Cas genetic circuits that interface host regulatory networks. *Mol. Syst. Biol.* **10**, 763, (2014).

10 Clamons, S. E. & Murray, R. M. Modeling Dynamic Transcriptional Circuits with CRISPRi. *bioRxiv*, 225318, (2017).

11 Lebar, T. *et al.* A bistable genetic switch based on designable DNA-binding domains. *Nat. Commun.* **5**, 5007, (2014).

12 Ma, H. *et al.* CRISPR-Cas9 nuclear dynamics and target recognition in living cells. *J. Cell Biol.* **214**, 529, (2016).

13 Jones, D. L. *et al.* Kinetics of dCas9 target search in *Escherichia coli*. *Science* **357**, 1420-1423, (2017).

14 Gander, M. W., Vrana, J. D., Voje, W. E., Carothers, J. M. & Klavins, E. Digital logic circuits in yeast with CRISPR-dCas9 NOR gates. *Nat. Commun.* **8**, 15459, (2017).

15 Samaniego, C. C., Subramanian, H. K. K. & Franco, E. Design of a bistable network using the CRISPR/Cas system. *IEEE Conf. Contr. Technol. Appl.*, 973-978, (2017).

16 Chen, P. Y., Qian, Y. L. & Del Vecchio, D. A Model for Resource Competition in CRISPR-Mediated Gene Repression. *IEEE Decis. Contr. P.*, 4333-4338, (2018).

17 Tan, C., Marguet, P. & You, L. C. Emergent bistability by a growth-modulating positive feedback circuit. *Nat. Chem. Biol.* **5**, 842-848, (2009).

18 Kiani, S. *et al.* CRISPR transcriptional repression devices and layered circuits in mammalian cells. *Nat. Methods* **11**, 723-U155, (2014).

19 Kiani, S. *et al.* Cas9 gRNA engineering for genome editing, activation and repression. *Nat. Methods* **12**, 1051-1054, (2015).

20 Menn, D. J., Pradhan, S., Kiani, S. & Wang, X. Fluorescent Guide RNAs Facilitate Development of Layered Pol II-Driven CRISPR Circuits. *ACS Synth. Biol.* **7**, 1929-1936, (2018).

21 Nissim, L., Perli, S. D., Fridkin, A., Perez-Pinera, P. & Lu, T. K. Multiplexed and Programmable Regulation of Gene Networks with an Integrated RNA and CRISPR/Cas Toolkit in Human Cells. *Mol. Cell.* **54**, 698-710, (2014).

22 Liu, Y. C. *et al.* Synthesizing AND gate genetic circuits based on CRISPR-Cas9 for identification of bladder cancer cells. *Nat. Commun.* **5**, 5393, (2014).

23 Gao, Y. C. *et al.* Complex transcriptional modulation with orthogonal and inducible dCas9 regulators. *Nat. Methods* **13**, 1043-1049, (2016).

24 Cress, B. F. *et al.* Rapid generation of CRISPR/dCas9-regulated, orthogonally repressible hybrid T7-lac promoters for modular, tuneable control of metabolic pathway fluxes in *Escherichia coli*. *Nucleic Acids Res.* **44**, 4472-4485, (2016).

25 Kim, H., Bojar, D. & Fussenegger, M. A CRISPR/Cas9-based central processing unit to program complex logic computation in human cells. *P. Natl. Acad. Sci. USA* **116**, 7214-7219, (2019).

26 Gardner, T. S., Cantor, C. R. & Collins, J. J. Construction of a genetic toggle switch in *Escherichia coli*. *Nature* **403**, 339, (2000).

27 Elowitz, M. B. & Leibler, S. A synthetic oscillatory network of transcriptional regulators. *Nature* **403**, 335-338, (2000).

28 Yeung, E. *et al.* Biophysical Constraints Arising from Compositional Context in Synthetic Gene Networks. *Cell Syst.* **5**, 11-24.e12, (2017).

29 Tsai, S. Q. *et al.* Dimeric CRISPR RNA-guided FokI nucleases for highly specific genome editing. *Nat. Biotechnol.* **32**, 569-576, (2014).

30 Butzin, N. C. & Mather, W. H. Crosstalk between Diverse Synthetic Protein Degradation Tags in *Escherichia coli*. *ACS Synth Biol* **7**, 54-62, (2018).

31 Kogenaru, M. & Tans, S. J. An improved *Escherichia coli* strain to host gene regulatory networks involving both the AraC and LacI inducible transcription factors. *J. Biol. Eng.* **8**, 2, (2014).

32 Santos-Moreno, J. & Schaerli, Y. A Framework for the Modular and Combinatorial Assembly of Synthetic Gene Circuits. *ACS Synth. Biol.* **8**, 1691-1697, (2019).

33 Basu, S., Gerchman, Y., Collins, C. H., Arnold, F. H. & Weiss, R. A synthetic multicellular system for programmed pattern formation. *Nature* **434**, 1130-1134, (2005).

34 Schaerli, Y. *et al.* A unified design space of synthetic stripe-forming networks. *Nat. Commun.* **5**, 4905, (2014).

35 Santos-Moreno, J. & Schaerli, Y. Using Synthetic Biology to Engineer Spatial Patterns. *Advanced Biosystems* **3**, 1800280, (2019).

36 Mangan, S. & Alon, U. Structure and function of the feed-forward loop network motif. *Proc Natl Acad Sci U S A* **100**, 11980-11985, (2003).

37 Wolpert, L. Positional information and pattern formation. *Curr. Top. Dev. Biol.* **6**, 183-224, (1971).

38 Filonov, G. S., Moon, J. D., Svensen, N. & Jaffrey, S. R. Broccoli: Rapid Selection of an RNA Mimic of Green Fluorescent Protein by Fluorescence-Based Selection and Directed Evolution. *J. Am. Chem. Soc.* **136**, 16299-16308, (2014).

39 Niederholtmeyer, H. *et al.* Rapid cell-free forward engineering of novel genetic ring oscillators. *eLife* **4**, e09771, (2015).

40 Potvin-Trottier, L., Lord, N. D., Vinnicombe, G. & Paulsson, J. Synchronous long-term oscillations in a synthetic gene circuit. *Nature* **538**, 514-517, (2016).

41 Rizzo, M. A., Springer, G. H., Granada, B. & Piston, D. W. An improved cyan fluorescent protein variant useful for FRET. *Nat. Biotechnol.* **22**, 445-449, (2004).

42 R Core Team. R: A language and environment for statistical computing. *R Foundation for Statistical Computing, Vienna, Austria*, (2017).

43 Schindelin, J. *et al.* Fiji: an open-source platform for biological-image analysis. *Nat. Methods* **9**, 676, (2012).